EXTENSIONS OF MENTER'S SST TRANSITION MODEL TO SIMULATE HYPERSONIC AND CROSS-FLOW TRANSITION

Zhang Xiaodong*, Gao Zhenghong*, Zhong bowen**
* Northwestern Polytechnical University, **Commercial Aircraft Corporation of China Ltd(COMAC)
zxd.nwpu@gmail.com;zgao@nwpu.edu.cn

Abstract

An improvement based on Menter's transition model has been made to expand its application in this paper. A compressibility correlation is added into the original model to simulate the hypersonic flow transition problem. The double wedge flat plate is numerically tested to validate the modified model, the computational results shows good agreement compared with the experiment data. Furthermore, a preliminary investigation of cross-flow instability on the NLF 0415 swept wing is made in the last section of this paper.

1 Introduction

Boundary layer transition phenomenon from laminar to turbulent has obvious impact on the characteristics of a flow field. fully laminar or fully turbulent can show marketable differences on skin friction , heat transfer and separation location, so the accuracy of the transition prediction will have great influence on the reducing aerodynamic drag of commercial aircraft and the design of the thermal protection system (TPS) of hypersonic reentry vehicle.

The process of transition depends on many factors, such as pressure gradient, free-stream intensity, Mach number, roughness, wall temperature etc. as the underlying physics of transition has not yet to be well understood by the boundary layer stability theory until now, some researchers turns to an alternative way to predict transition. Since a large amount of transition data is available from flight test and wind tunnel experiments, empirical method could be formulated that can reliably predict transition process. In 2004 Langtry and Menter[1][2] developed a correlation-based transition model using local variables which coupled with SST k- turbulent model. This method combines the advantages of low Reynolds number turbulence model and the transition empirical correlation, and forms a framework for implementation of transition correlations applying local variables to general-purpose CFD(computational Fluid Dynamics) methods.

However the transition correlations in this model are originally from a low-speed, 2-D incompressible flat plate transition experiment, without further consideration of the Mach number and three-dimensional transition mechanisms, hence this model need to be modified and extend to solve the supersonic/hypersonic[4][5] [6] and 3D sweep wing transition problem.

In the first section various transition types and several parameters that dominate the boundary layer transition will be discussed briefly. In the second section, a compressibility correlation based on the experiment data is introduced into the original model. The flow field over double wedge flat plate was numerically simulated to test the improved model and got reasonable result compared with the experiment data. at last, the author analyzed the flow-field character of NLF 0416 sweep wing, and finally gave a preliminary discussion on how to implement the cross-flow instability

into the original framework.

2 The transition mode

There are several instability mechanisms(see below) in the swept wing boundary layers. Each of these instabilities is characteristic for specific conditions.
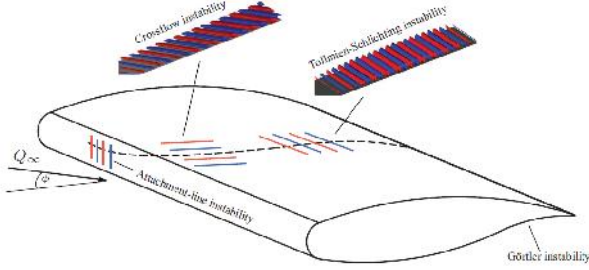

Fig.1 various instability mechanisms on swept wing boundary layer

- The nature transition which is often referred to as TS(Tollmien Schlichting)instability, this transition mode happens at low free-stream turbulence levels (<1%), adverse pressure gradients have a destabilizing effect.

- The separated flow transition occurs in the shear layer of the separated laminar boundary layer flow as a result of the in-viscid instability mechanism.

- Görtler vortices transition is caused by in-balance between centrifugal force and pressure gradient, this is a form of centrifugal boundary layer instability only happening on concave surface. this type of transition happens when Görtler number is greater than 7.

$$Go = \mathrm{Re}_{\theta t} \sqrt{\theta/r} \geq 7$$

- Cross-flow [8][9] instability usually dominates the three-dimensional boundary layer transition over the swept wing. the cross-flow velocity is zero both at the boundary layer edge and at the wall, such that the S-shaped cross-flow velocity profile has an inflection point and is in-viscidly unstable. unlike the TS instability, favorable pressure gradients have a destabilizing effect. a connection between attachment-line and cross-flow disturbances was found from the computation by Mack.

- The attachment line instabilities may be found in the boundary layer forming along the attachment line of a sweep wing, this instability could be stable with decreasing leading edge radius and sweep angle. Poll[10] proposed that when the attachment-line Reynolds number

$$\mathrm{Re}_{\theta al} = 0.404 \sqrt{\frac{U_\infty r \sin^2 \Lambda}{2\in \cos \Lambda}}$$ is great than

240,the attachment line transition will occur.

The onset of transition is mainly affected by the pressure gradients and free-stream turbulence intensity, but there are some other parameters such as the effect of compressibility, wall temperature, surface roughness and leading edge radius et al, that will also affect the transition process. For example: increasing Me (on an adiabatic wall) exerts a strong stabilizing effect; Wall cooling (respectively wall heating) is stabilizing (respectively destabilizing) in air.

3 A brief description on the $x - \overline{\mathrm{Re}_{\theta t}}$ transition model

The $x - \overline{\mathrm{Re}_{\theta t}}$ model is based on two transport equations: one for intermittency   and one for a transition onset criterion in term of local momentum thickness Reynolds number $\overline{\mathrm{Re}_{\theta t}}$.The intermittency   equation indicates the time ratio of the turbulent or laminar flow, which is used to control the onset and the transition process.

$$\frac{\partial (\rho x)}{\partial t} + \frac{\partial (\rho U_j x)}{\partial x_j} = P_x - E_x + \frac{\partial}{\partial x_j}[(\mu + \frac{\mu_t}{\sigma_f})\frac{\partial x}{\partial x_j}] \quad (1)$$

$$P_x = c_{a1} \rho S F_{length} F_{onset}^{0.5} x^{0.5}(1 - c_{e1}x)$$

$$E_x = c_{a2} \rho \Omega F_{turb} x (c_{e2}x - 1)$$

$$F_{onset} = \max(F_{onset2} - F_{onset3},0)$$

$$F_{onset2} = \min(\max(F_{onset1}, F_{onset1}^4),2.0)$$

$$F_{onset3} = \max(1 - (R_T / 2.5)^3,0)$$

$$F_{turb} = e^{-(R_T/4)^4} \qquad F_{onset1} = \mathrm{Re}_v \Big/ \mathrm{Re}_{\theta c}$$

$$F_{length} = Re_{LT}/(qc/\,)$$

$$Re_c = \overline{Re_t}\left(-1.5546\times10^{-7}\overline{Re_t}^2 - 2.7776\times10^{-4}\overline{Re_t} + 0.97505\right)$$

$$Re_{LT} = 7.5537\times10^{13}\overline{Re_t}^{-2.9}$$

The $\overline{Re_{,t}}$ equation is designed to introduce the free-stream information into the boundary layer as the criterion of transition onset position, which realizes its localizable process.

$$\frac{\partial(\ldots\overline{Re_{,t}})}{\partial t} + \frac{\partial(\ldots U_j\overline{Re_{,t}})}{\partial x_j} = P_{,t} + \frac{\partial}{\partial t}[\dagger_{,t}(\sim + \sim_t)\frac{\partial\overline{Re_{,t}}}{\partial x_j}] \quad (2)$$

$$P_{,t} = c_{,t}\frac{\cdots}{t_{scale}}\left(Re_{,t} - \overline{Re_{,t}}\right)\left(1 - F_{,t}\right)$$

$$F_{,t} = \min\left(\max\left(F_{wake}\cdot e^{-\left(\frac{y}{u}\right)^4},1-\left(\frac{x-1/c_{e2}}{1.0-1/c_{e2}}\right)^2\right),1\right)$$

$$u = u_{BL}50\Omega d/q,\; u_{BL} = 7.5_{''BL}$$

$$_{''BL} = \overline{Re_{,t}}\sim/\ldots q,\; F_{wake} = e^{-\left(Re_{\check{S}/10^5}\right)^2}$$

$$Re_{\check{S}} = \ldots\check{S}d^2/\sim$$

Finally, the effective intermittency obtained from the above is used to control the production term in the K-equation of the SST turbulence model to simulate the transition process in the end.

$$\frac{\partial\ldots k}{\partial t} + \frac{\partial\ldots U_jk}{\partial x_j} = \tilde{P}_k - \tilde{D}_k + \frac{\partial}{\partial x_j}(\sim + \dagger_k\sim_t\frac{\partial k}{\partial x_j})$$

$$x_{eff} = \max(x,x_{sep}),\quad \tilde{P}_k = x_{eff}P_k$$

$$D_{k,eff} = \min(\max(x_{eff},0.1),1)D_k \quad (3)$$

the model constants are:

$$\dagger_{,t} = 2.0,\; c_{,t} = 0.03,\; c_{e2} = 50,\; c_{e1} = 1.0,$$

$$c_{e2} = 50,\; c_{a1} = 2.0,\; c_{a2} = 0.06,\; \dagger_x = 1.0。$$

4 The modification of the $x - \overline{Re_{,t}}$ model for hypersonic transition flow

In $x - \overline{Re_{,t}}$ transition model, the onset of transition process is controlled by an empirical correlation for transition momentum thickness onset Reynolds number $Re_{,t} = f(Tu,\})$ as a function of turbulence intensity *Tu* and pressure gradient , the definition is as follows:

$$Re_{,t} = f(Tu,\}_{,}) = E(Tu)F(\}_{,})$$

$$E(Tu) = [1173.51 - 589.428Tu + \frac{0.2196}{Tu^2}],Tu \le 1.3$$

$$E(Tu) = 331.50[Tu - 0.5658]^{-0.671},Tu > 1.3$$

$$F(\}_{,}) = 1 - [-12.986\}_{,} - 123.66\}_{,}^2 - 405.689\}_{,}^3]e^{-\left[\frac{Tu}{1.5}\right]^{1.5}},\}_{,} \le 0$$

$$F(\}_{,}) = 1 + 0.275[1 - e^{[-35.0\}_{,}]}]e^{\left[\frac{-Tu}{0.5}\right]},\}_{,} > 0$$

$$\}_{,} = (_{''}^2/\varepsilon)/(dU/ds) \quad (4)$$

As this correlation is originally obtained from in-compressible flat plate transition experiments, it is inappropriate to use this transition model in the hypersonic problems. The transition onset momentum thickness $Re_{,t}$ will increase from 600 to 1300 as the Ma number increases from 1 to 12, which is found in hypersonic smooth sharp cones transition experiments of Langley wing tunnel[6]. This means the onset of transition process in the boundary layer will be triggered earlier while using the original correlation. it is also reported that a possible 8-30% increase on the length of transition as Mach number increases. since F_{length} controls the production term of the intermittency equation, the transition length will increases as F_{length} decrease. this model do not consider too much physical mechanisms, the difference between first and second mode was not accounted in here.
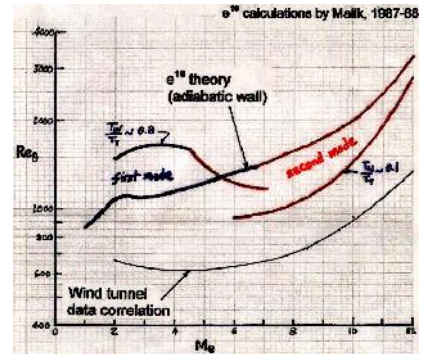

Fig.2 The transition experiment on sharp cone $Re_{,}$ $VS. M_e$

The authors in this paper introduces the local Ma effect into the original $Re_{,t}$ correlation and F_{length} term based on hypersonic wind tunnel transition experiments, the modified correlation is expressed as follows:

$$Re_{,t} = C(Tu,\}_{,},Ma) = E(Tu)F(\}_{,})G(Ma)$$

$$G(Ma) = (1 + 0.3*Ma^{0.6})^{0.5}$$

$$F_{length} = F_{length}/(1 + 0.25Ma^{0.635})\quad Ma\in[0,8] \quad (5)$$

In order to validate this correlation, a hyper double wedge flat will be numerically investigated in this paper. Thomas Neunhahn and Herbert Olivier investigated the influence of the leading edge radius and the wall temperature on the hypersonic boundary layer of a double wedge flat in Aachen University TH2 hypersonic shock tunnel in 2006. The inlet conditions for the performed experiments are given in Table 1.

Table 1 Inlet conditions at leading edge plate

Ma_∞ [-]	8.1
P_∞ [mbar]	5.2
$\cdots_\infty$ [kg/m^3]	0.0171
$T_\infty[K]$	106
U_∞ [m/s]	1635
$Re_{x,\infty}[1/m]$	3.8e6
Tu%[-]	0.5%
$\Delta t_{test}[ms]$	2.0
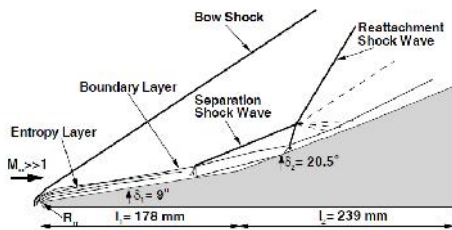
Fig. 3：Shock / boundary layer interaction schematic on a blunt

double wedge configuration

The first ramp has an angle of 9° and the second one 20.5°. The length of the first ramp is L=180 mm, and the second one is 250 mm. Neunhahn selected the first ramp leading radius in the experiment as 0mm(sharp leading edge),0.5mm and 1mm respectively (see Figure 3).

The Lower-Upper Symmetric Gauss-Siedel (LU-SGS) scheme is adopted for implicit inversion of the linear system of equations. The Roe flux-difference schemes is used for calculating in-viscid fluxes and a second-order central scheme is used to discretize the viscous terms. The third-order MUSCL scheme is used for spatial reconstruction.

The H-grid is adopted for the sharp leading edge case whereas the C-grid is adopted for the blunt leading edge case. the computation grid and the inlet condition setting are shown in figure 4-5. the y^+ is between 0. 1~0.5 for the accuracy of transition prediction.

The inlet condition for $\overline{Re}_{x,t}$ should be changed as the introduction of Ma correlation, the boundary condition of $\overline{Re}_{x,t}$ is obtained by taking $Tu_{inlet}, Ma_{inlet}, \}_x = 0$ in formula (5).
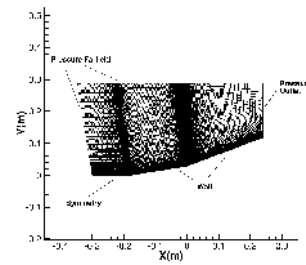

Fig. 4 Grid and boundary conditions
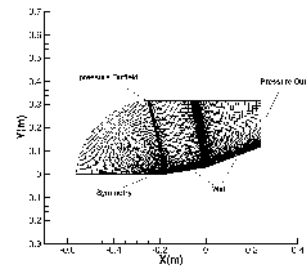for sharp leading edge

Fig. 5 Grid and boundary conditions
for blunt leading edge

Figure 6 shows the comparison of surface pressure coefficients using various models respectively in sharp leading edge case under wall temperature $T_w = 300K$. The separation region is predicted a little smaller by the Menter's original transition model; owing to the onset value of transition obtained by the in-compressive correlations is lower compared to the value in the hypersonic condition, which will trigger transition earlier. The early transition results in the deficiency of simulating separation zone. As the new correlation will increase the onset value of transition in the hypersonic condition, the computed surface pressure distribution matches with the experiment better. Small differences can be identified due to some side-flow that occurs in the experiment. the pressure coefficient predicted by the laminar

model also fit the experiment data well from the figure 6,but the laminar model fail to predict the transition phenomenon existing in the case. It is easy to see the SST turbulent model can't capture the separation phenomenon in the inflexion point, see Figure 7. This is because that the SST turbulent model is designed for the turbulent boundary layer, the transition occurs very quickly before the flow arrives to the second ramp, and the turbulent boundary layer will undergo more adverse pressure to separation, so it is not unusual the SST model cannot predict this separation phenomenon in the inflexion point.
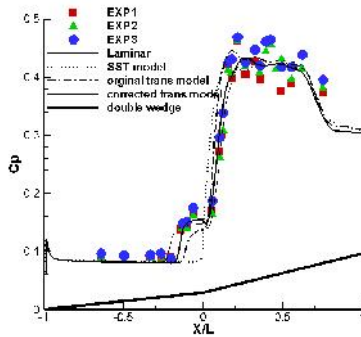
Fig. 6 the Cp comparison of experiment and different models for $R_n = 0mm\ T_w = 300K$
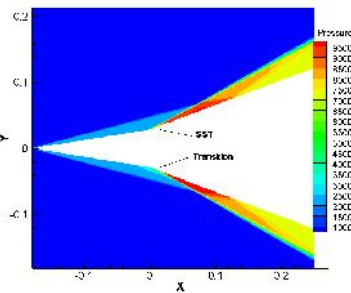
Fig. 7 The difference of pressure contour computation result between the SST and the transition model

Figure 8 shows the transition model could capture this shock wave/boundary layer interaction induced separation phenomenon, which brings notable change of the pressure near the inflexion point. Figure 9 is a schlieren image of the shock boundary layer and the separation zone in the whole flow field from the experiment.
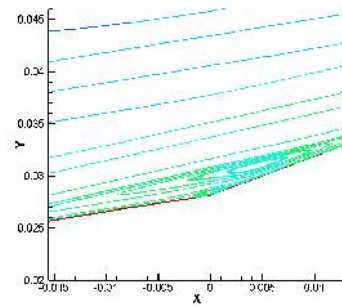

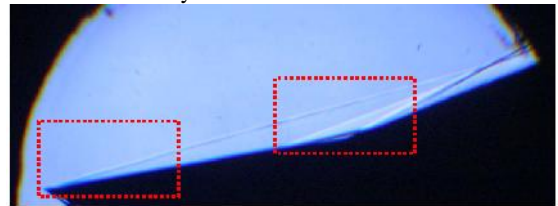Fig. 8 The separation zone predicted by the transition model

Fig. 9 Schlieren image of the shock boundary layer and separation in the whole flow field

The influence of different leading edge radius on pressure coefficient under wall temperature $T_w = 300K$ is demonstrated in figure 10. It shows that the separation length of separation bubble increases as the radius of the leading edge changes from sharp to 0.5mm. Further increasing of the leading edge radius does not affect the separation bubble length apparently.

The pressure coefficient for the sharp leading edge case increases much rapidly than the other two blunt cases after the boundary layer is separated in the inflexion point. The computational results agree well with the experiment.
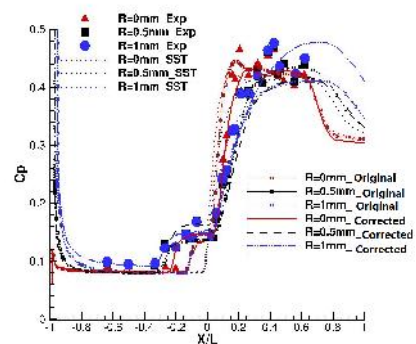

Fig. 10 Effect of different leading edge radii under wall temperature 300K on the pressure distribution

The turbulent flow reattaches to the wall at the beginning of the second ramp, which was found in the experiment. Because of the intense compressibility effect in the second ramp, the

aerodynamic heat rises very quickly (see Fig.11). As the transition process has already finished in the separation region, turbulence enhances the heat exchange in the boundary layer (Fig.12). Considering those factors it's not surprising that a great change in the temperature field occurs at the beginning of the second ramp.
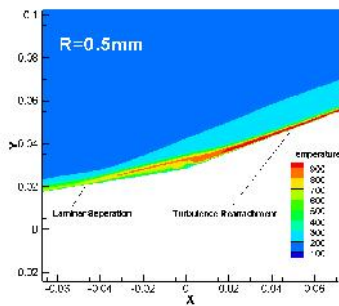

Fig. 11 Temperature flow-field in the inflexion point for the case of 0.5 mm leading edge radius
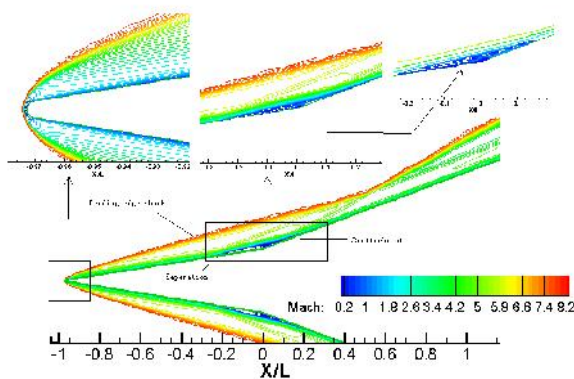

Fig. 12 Shock / boundary layer interaction phenomenon for $R_n = 0.5mm$ under wall temperature $T_w = 300K$

5 A preliminary discuss on cross-flow transition

The cross-flow vortices develop in the swept-wing three-dimensional boundary layer, its direction is perpendicular to the stream-wise direction of the external flow. The cross-flow profile results from the combined effect of pressure gradient and sweep angle which leads to a curved streamline in the outer in-viscid flow. Inside the boundary layer the pressure gradient remains constant while the stream-wise velocity reduces to zero at the wall. This leads to an imbalance of centrifugal and pressure forces which creates a cross-flow inside the boundary layer towards the concave side of the external streamline. see figure 13.
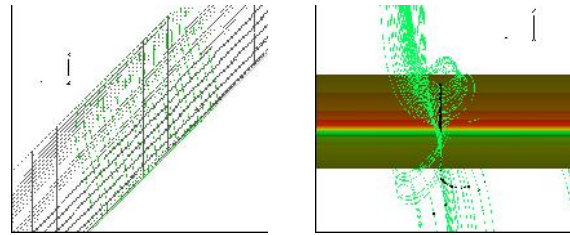

Fig. 13 The streamline over the infinite 45° sweep NLF-0415 wing

Two types of cross-flow instabilities need to be distinguished: the stationary cross-flow waves and the travelling cross-flow waves. they are generated by different receptivity mechanisms. Stationary cross-flow disturbances are excited directly by steady surface variations (surface polishing or suction). Travelling cross-flow waves require an unsteady source such as free-stream turbulence, but the receptivity mechanisms probably differ from those for TS waves. The relative importance of stationary and travelling cross-flow modes depends on the relative importance of steady and unsteady excitations. The general idea for cross-flow induced transition is that stationary cross-flow waves dominate in free flight conditions and in very low free-stream disturbance wind tunnels, while travelling cross-flow waves play the major role in more classical wind tunnels.

Most of the early work on predicting the cross-flow transition is mainly on e-N method. Cornelia Seyfert and Andreas Krumbein in DLR developed a method which could couple with the original SST $\gamma - \overline{Re_{,t}}$ model to predict the cross-flow transition in 2012. the core idea is using the cross-flow vorticity Reynolds number as an indicator, this leads to:

$$\text{Re}_{v.y} = \frac{...d^2}{\sim} \left| \frac{\partial v}{\partial z} \right| \qquad (6)$$

The second step is to find a threshold to determine if the cross-flow transition occurs or not, A lot of researchers have conducted a fundamental experiments investigation on swept cylinder or swept wing. some cross-flow criterion have been proposed based on experiment observation.

The first criterion is $\text{Re}_{cf} = W_{max} u_{10} / v_e$, where the W_{max} is the maximum of the cross-flow velocity component, u_{10} is the height above the wall to the surface where the cross flow velocity

drop to 10% of W_{max}, the cross-flow transition happens when Re_{cf} exceeds 165.

The second criterion is proposed by Coustols, the cross-flow transition occurs when the Reynolds number based on the stream-wise displacement thickness Re_{u2t} becomes lager than a critical value Re^*_{u2t} which is a function of the shape factor H. this criterion reads:

$$Re^*_{u2t} = 95.5 \arctan\left(\frac{0.106}{(H-2.3)^{2.052}}\right) \quad 2.3 < H < 2.61$$
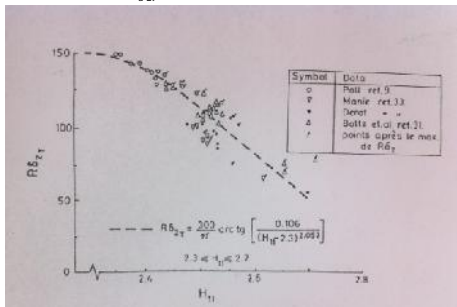
$$Re^*_{u2t} = 150 \quad H < 2.3 \tag{7}$$

Fig.14 Cross-flow criterion Re_{u2t} versus shape factor H

It is important to keep in mind that the use of this criterion is restricted to accelerated flows in the vicinity of the leading edge of the swept wings. Large values of Re_{u2} can be reached in decelerated flows downstream of the point of minimum pressure. This criterion was recently improved in order to take into account compressibility effects; Re_{u2} was simply replaced by $Re_{u2t}/(1+0.2\,M_e^2)$.

The shape factor H depends on streamwise quantities only and an approximation as a function of the pressure gradient parameter . Because the pressure gradient parameter is already part of the -Re $_t$ model, the shape factor H is directly accessible.
H =1000*(3.6268* $}_{''}$ ^{4}-0.4118* $}_{''}$ ^{3}+0.0098* $}_{''}$ ^{2}-0.0034* $}_{''}$ +0.00261)   (8)

The cross-flow instability was trigged when the ratio of cross-flow vorticity Reynolds number and stream-wise displacement thickness exceed a value f. The final local to non-local Reynolds-number correlation which is used for the prediction of transition due to cross-flow instabilities is:

$$\frac{Re_{v.y}}{Re_{u2t}} = f(local\ evaluated\ FSC\ equation) \tag{9}$$

The right hand side of the ratio is not a constant as is the case for the stream-wise Reynolds number correlation. Nevertheless, it is possible to evaluate this ratio locally. the approximate solution of the three-dimensional boundary-layer equations according to Falkner-Skan-Cooke (FSC) is used which leads to a system of ordinary differential equations to determine the f.
The Falkner-Skan-Cooke Equation is :

$$F''' + FF'' + S_H[1-(F')^2] = 0$$
$$g'' + Fg' = 0 \tag{10}$$

where S_H is Hartree-parameter, the definition is $S_H = 2m/(m+1)$. the solution of this equation is :

$$u(y) = F'\cos^2{}_{''} + g\sin^2{}_{''}$$
$$w(y) = (g - F^2)\cos{}_{''}\sin{}_{''}$$

After the velocity profile is solved, the cross-flow vorticity $Re_{v,y}$ and the displacement Reynolds number Re_{u_2} could be linked finally.

In order to implement this cross-flow instability into the existing $X - \overline{Re_{,t}}$ framework, the modification in the source term of the equation is needed. the CF instability and TS instability could compete with each other, and determine which transition mechanism will occurs when its criterion is satisfied. the new equation is expressed as follows:

$$\frac{\partial(...X)}{\partial t} + \frac{\partial(...U_jX)}{\partial x_j} = P_X + P_{X\_cf} - E_X + \frac{\partial}{\partial x_j}\left[(\sim + \frac{\sim_t}{\dagger_f})\frac{\partial X}{\partial x_j}\right]$$

P_{X_cf} have a similar expression with the P_r, which lead to:

$$P_{X\_cf} = c_{a3}...S[F_{onset\_cf}X]^{c_{r3}}(1 - c_{e3}X)$$

$$F_{onsetcf1} = \frac{Re_{v.y}}{Re_{u2t}*f}$$

$$F_{onset\_cf} = \max(F_{onsetcf2} - F_{onset3}, 0)$$

$$F_{onsetcf2} = \min(\max(F_{onsetcf1}, F_{onsetcf1}^4), 2.0)$$

$$c_{e3} = 1.0 \quad c_{r3} = 0.5$$

c_{a3} controls the strength of the cross-flow instability in the production term. it is stressed that the F_{onset_cf} term should be deactivate in the adverse pressure gradient region because the Re_{u2t} criterion is only valid to the accelerated

flows.

The infinite swept NLF(2)-0415 wing is adopted to validate the corrected model, this experiment is conducted by J.Ray Dagenhart and William S.Saric in the Arizona state university wing tunnel. the geometry sweep angle is 45°, the angle attack is -4°. The Reynolds number varied between $1.93*10^6$-$3.73*10^6$. its small leading-edge radius eliminates the attachment-line instability mechanism. the Görtler instability is not present because no concave regions are on the upper surface. the cross-flow is driven strongly by the favorable pressure gradient near the leading edge at the negative angle. the minimum pressure point on the upper surface at all the condition is at 0.71 chord . see figure15.
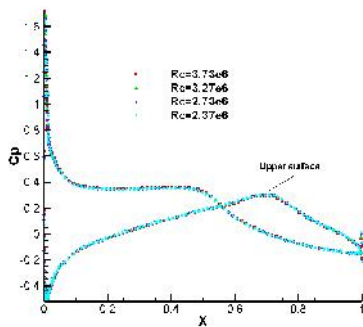

Fig.15 the pressure distribution at different Reynolds number

Since the original $x-\overline{Re}_{,t}$ model only consider the effect of the turbulence intensity and the pressure gradient, the transition process normally occurs when the favorable pressure gradient turns to adverse pressure gradient on the wing surface. as figure 16 shows that the transition occurs near the 71% chord predicted by the original $x-\overline{Re}_{,t}$ model.
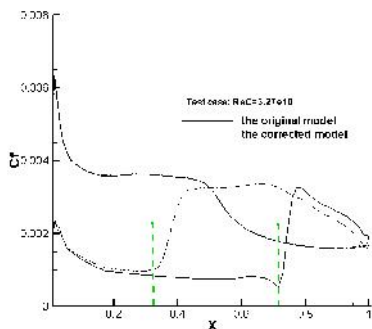

Fig.16 the skin friction coefficient around mid section of the wing

After introducing the cross-flow instability

mechanisms, the transition location predicted by the corrected $x-\overline{Re}_{,t}$ model could agree well with the experiment data. the green line indicated the transition onset position. the final results of the corrected model and original model versus the experimental data are plotted as below.
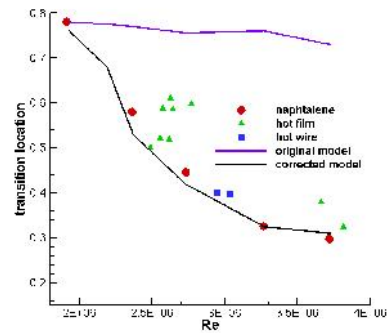

Fig.17 the transition location on the infinite swept wing

6 Conclusions

The $x-\overline{Re}_{,t}$ transition model do not try to model the physical of the flow, but to build a framework for the implementation of correction-based model into general-purpose CFD methods. therefore this model is essentially relied on the accuracy of empirical correlations. After introducing a new compressibility correlation and taking account the cross-flow instability, the modified $x-\overline{Re}_{,t}$ model could extend to the hypersonic transition flow and 3D crossflow induced transition flow. the application of the modified $x-\overline{Re}_{,t}$ model to the flow over double wedge flat plate and infinite 0415 swept wing shows good agreement with the experiment data. the proposed model still has much room to improve for the engineering applications. this transition model are of good value in the future aerodynamic design and CFD transition prediction.

References

[1] Menter F R, Langtry R B, Likki S R, Suzen Y B, Huang P G and Völker S. A Correlation Based Transition Model Using Local Variables Part 1:

Model Formulation. *Journal of Turbomachinery*, 128(3): 413–422, 2006.

[2] Langtry R B, Menter F R, Likki S R, Suzen, Y B, Huang P G and Völker S. A Correlation Based Transition Model Using Local Variables Part 2: Test Cases and Industrial Applications. *Journal of Turbomachinery*, 128(3): 423–434,2006.

[3] Robin B Langtry, Florian R menter. Correlation-Based Transition Modeling for Unstructured Parallelized Computational Fluid Dynamics Codes, *AIAA Journal*,47(12):2894-2906, 2009.

[4] Thomas Neuenhahn , Herbert Olivier. Influence of the wall temperature and the entropy layer effects on double wedge shock boundary layer interactions, *AIAA 2006-8136*,2006

[5] Horvath T J, Berry S A, Hollis B R, Chang C L, Singer B A. Boundary layer transition on slender cones in conventional and low disturbance mach 6 wind tunnel, *AIA- 2002-2743*, 2002.

[6] Eli Reshotko. Is Re_θ / M_e a Meaningful Transition Criterion?. *AIAA -2007-943*, 2007.

[7] Cliquet J, Houdeville R, Arnal D, Application of Laminar-Turbulent Transition Criteria in Navier-Stokes Computations, *AIAA Journal,* Vol. 46, No. 5, pp. 1182-1190, 2008.

[8] Dagenhart J R, Saric W S, Crossflow Stability and Transition Experiments in Swept-Wing Flow, NASA report, *TP-1999-209344*, 1999.

[9] William S Saric and Helen L Reed, Crossflow instablities- Theory &Techology , *AIAA 2003-771*,2007.

[10] Poll DIA. Some observations of the transition process on the windward face of a long yawed cylinder. *J. Fluid Mech.* 150:329-56, 1985

Copyright Statement